

MICROGRAVITY CONTAINERLESS PROCESSING IN LONG DROP TUBES

by

R. J. Bayuzick, N. D. Evans, and W. H. Hofmeister
Vanderbilt University
Nashville, Tennessee 37235

and

M. B. Robinson
Space Science Laboratory
Marshall Space Flight Center, Alabama 35812

ABSTRACT

Extensive experience in utilizing long drop tubes for studying effects of microgravity on the solidification of alloys has been obtained. While some modifications are necessary to improve versatility, the facility has proven to be most useful.

Both an electron beam furnace and an electromagnetic levitation furnace can be used. The electron beam furnace is used with vacuum environments (10^{-5} torr) whereas the levitation furnace is presently used only in inert gas environments (above 100 torr). Experiments are best applied to refractory alloys because of the sensitivity of the detectors now being used to observe solidification. Processing of lower melting point metals and alloys simply cannot be recorded. On the other hand, expected improvements in detector sensitivity will allow experimentation with relatively low melting alloys. In such cases, solidification will occur in flight only if higher inert gas pressure is used (100 to 760 torr) to increase heat loss by convection. Under these conditions microgravity conditions no longer apply.

However, as shown by results to date, it is not microgravity as such that is important in drop tube solidification. Instead it is the containerless nature of the process that is significant, leading to large degrees of undercooling before solidification and therefore unique alloys.

INTRODUCTION

The one hundred meter drop tube has been used to successfully drop about seventy Nb-Ge alloys. In this context, successfully means that large undercooling was obtained before solidification occurred. These experiments, in conjunction with previous work involving the 30 meter drop tube [1-4], have shown that a drop tube is a most useful facility for studying the effects of microgravity containerless processing and low gravity containerless processing on solidification.

Several different alloy compositions in the Nb-Ge system have been studied. Namely, results have been obtained on alloys with nominal compositions Nb-13 at% Ge, Nb-18 at% Ge, Nb-22 at% Ge, Nb-25 at% Ge, Nb-27 at% Ge, and Nb-37 at% Ge. Some typical results for

Nb-25 at% Ge are presented here. It is instructive, in fact necessary, to compare the drop tube results to arc cast results and to the results of "normal" rapid solidification by liquid quenching. It is necessary because ultimately the advantages and disadvantages of microgravity containerless processing on earth as well as materials processing in space must stand against the more commonplace methods of solidification.

DROP TUBE HARDWARE

The drop tube can accommodate any furnace that can be adapted to the bell-jar atop the facility. To date two furnaces have been successfully used to heat, melt and release samples into the drop tube for processing.

The electron bombardment, or E-beam, furnace employs a heated tungsten filament which emits electrons by thermionic emission. Since the filament is held at a negative 5 kV potential, the emitted electrons will bombard and heat the grounded sample. The sample is grounded through a tungsten support wire. One disadvantage of the E-beam furnace is that it must be operated in hard vacuum (10^{-5} torr) and is therefore limited to higher melting temperature alloys ($T_m > 1600$ K) since the samples falling in vacuum are cooled solely by radiative heat loss. There is therefore not sufficient free fall time to undercool samples significantly before impact. To process lower temperature alloys at a higher cooling rate, an electromagnetic levitation furnace is used. The E-M levitator is powered by a 10 kW Lepel unit operating at 100 KHz. For both furnaces, the sample thermal history is recorded by an optical pyrometer before sample release into the drop tube.

Infrared detectors are used to monitor drop brightness and to sense recalescence events. Three United Detector Technology UDT450 silicon detector/amplifiers are positioned at the 40 and 264 ft levels as well as the uppermost (350 ft) level as shown in Figure 1. According to specifications, the detectors are sensitive to light from the 9660 to 2635 K (0.3 to 1.1 μm) range. However, recalescence events have been detected when nucleation occurred as low as 1750 K (1.66 μm) in the Nb-Ge alloys. During recalescence, the heat of fusion raises the drop temperature enough so that the low wavelength end of the emitted spectrum is within the detector's sensitivity range. In practical terms this means that, with the present experimental arrangement, recalescence in metals and alloys whose equilibrium freezing points are less than 1700 K cannot be observed.

Figure 2 shows the detection of recalescence in a Nb-25 at% Ge alloy. The brightness detected is measured as a function of fall time down the tube. The sharp increase in brightness at around 1.2 seconds was due to solidification at an undercooling of 242 K (about 11% below the liquidus) and therefore recalescence. The actual temperature reached, i.e., just before recalescence, was about 1920 K.

DROP TUBE MECHANICS

In order to gain insight into the cooling capabilities of the drop tube, calculations have been performed on several pure materials. The techniques follow those of Robinson [4] and Wallace [5]. These calculations estimate the final temperature of a liquid drop released at its melting temperature and undercooled for the entire 100 meter free fall. Assuming a spherical shape, the heat loss can be expressed as [6]

$$dQ/dt = - \epsilon A \sigma (T^4 - T_0^4) - hA(T - T_0) \quad (1)$$

where dQ/dt is the time rate of heat loss, ϵ is the emissivity of the sample, A is the area of the spherical drop, σ is the Stefan-Boltzmann constant, h is the convective heat transfer coefficient, T is drop temperature and T_0 the ambient temperature.

Determination of the temperature requires a knowledge of the specific heat of an undercooled liquid metal. The heat capacity of undercooled metals has been found in some cases to rise continuously [7] but data are unavailable for most materials of interest. For the purpose of these calculations the heat capacity was assumed constant and equal to the liquid heat capacity of the melting temperature. Nucleation and growth of the solid phase will terminate the undercooling of the materials before the limit of undercooling in the drop tube is reached. The calculations reflect the maximum undercooling possible in the absence of solidification.

The three masses used in the calculations represent the limit of sizes possible with present drop tube furnaces. Masses from 0.070 to 0.140 grams have been dropped from the E-beam furnace in vacuum conditions. Electromagnetic levitated samples from 0.2 to 0.5 grams have been successfully dropped in helium atmospheres. In vacuum conditions h is zero and cooling is accomplished by radiation alone. Since the temperature dependence of the emissive term in equation one is to the fourth power, it is not surprising that lower melting point materials will undercool very little in vacuum. Inert atmospheres of increasing pressure increase the importance of the convective term, the second term of equation one, and allow large undercooling in lower melting metals.

Undercooling has been normalized to the hypercooling temperature. Calculations of heat flow in solidifying drops have shown that for conditions similar to the drop tube ($h \leq 10^3$ K/sec, Biot number < 0.1) the solidifying interface will recalesce to the melting temperature unless the hypercooled regime is achieved [8]. The hypercooling temperature for the pure metals considered has been estimated as (after Hirth) [9]:

$$T^* = \Delta H/C_p \quad (2)$$

where ΔH_f is the heat of fusion at the usual freezing point (T_m) and C_p is the heat capacity for the liquid metal. Table 1 lists the calculated hypercooling temperatures.

The results of the calculations for vacuum, 200 torr He, and 760 torr He are shown graphically in Figures 3, 4 and 5 respectively. Note that in vacuum only metals and alloys whose freezing points are above 2000 K can be hypercooled and even then only if the drop mass is about 70 milligrams. At 200 torr the hypercooling can be achieved with metals whose melting point is about 900 K as long as the drop mass is less than 200 milligrams. With 760 torr He there is no problem with hypercooling low melting metals and alloys even with drop sizes as large as 500 milligrams.

The above results show that it would be necessary in some cases to use an atmosphere in the drop tube in order to obtain significant undercooling before impact at the bottom. Hence, it would obviously be required to know the drag force on the drops in such experiments.

The drag force on drops was calculated for Nb-27 at% Ge drops of three different masses at helium pressures from 100 to 800 torr and expressed as a fraction of earth gravity. Spherical liquid drops were assumed to be released at the melting temperature and allowed to undercool for 100 meters. At the end of free fall the velocity, Reynolds number and gas properties were noted. The drag coefficient was determined from White's empirical curve fit for spheres [11],

$$C_D = 24/Re + 6/(1+R3) + 0.4 \quad (3)$$

where C_D = drag coefficient and Re is the Reynolds number. The drag coefficient is then used according to the method of Incropera and DeWitt [12] to determine the drag force as:

$$F_D = C_D A \rho V^2 / 4 \quad (4)$$

where F_D is the drag force, A is the area normal to the free stream, ρ is the density of the gas at the thin film temperature, and V is the velocity of the drop. The radii of the drops are: 0.2 grams = 1.8 mm, 0.5 grams = 2.5 mm, 5 grams = 5.4 mm. The drag forces as a function of size and pressure are shown in Figure 6.

EXPERIMENTAL RESULTS

Deep undercooling has been obtained in a variety of Nb-Ge alloys. A summary of the undercooling is given in Figure 7; the temperatures at which recalescence was observed to occur are superimposed on the Nb-rich portion of the Nb-Ge phase diagram. Undercoolings ranged from 3% and 6% (about 40 K and 100 K respectively below the liquidus) in two separate Nb-25 at% Ge specimens to 31% (about 760 K) below the liquidus in a Nb-16 at% Ge specimen. A number of specimens, each of different Ge composition, undercooled to about 25% of the liquidus but the most common experience was for undercooling to about 20% of the liquidus.

Microstructural analysis by x-ray diffraction, optical microscopy, and scanning electron microscopy with energy dispersive analysis has been done in each case. Some results for Nb-25 at% Ge specimens in the as-dropped undercooled condition are presented below and compared to specimens in the arc cast condition and the liquid quenched condition.

Arc Cast Nb-25 at% Ge

Arc cast on a water cooled copper block, this alloy has a matrix of γ particles (35 at% Ge) having a bimodal size distribution, which are surrounded by a continuous β phase (19.8 at% Ge). By volume, the matrix is 64% β , 33% large ($38.8 \mu\text{m} \times 9.4 \mu\text{m}$) γ particles, and 3% small ($5.4 \mu\text{m} \times 3.7 \mu\text{m}$) γ particles. This alloy is shown in Figure 8.

Drop Specimen NT008

This specimen was melted in the electron-beam furnace, dropped in a vacuum (10^{-5} torr), and quenched in oil. It has an actual composition of Nb-26.5 at% Ge. The specimen undercooled 450 K ($\Delta T/T_m = 0.22$).

Shown in Figure 9, approximately 77% of this specimen consists of finely dispersed γ particles (35 at% Ge) in a continuous β phase (22 at% Ge). Here, these regions appear dark.

By volume, these particles comprise 41% of the fine regions and are approximately $4.6 \mu\text{m} \times 1.5 \mu\text{m}$ in size. A higher magnification of a fine region is shown in Figure 10.

The remaining 23% of the specimen has a coarsened structure, appearing as the light regions in Figure 9. These regions have enlarged γ particles (36.4 at\% Ge , $13.8 \mu\text{m} \times 3.6 \mu\text{m}$) in a continuous β phase (20.5 at\% Ge). These particles comprise 31% of the coarsened regions. It is thought that the coarsening is caused by localized reduced solidification rates due to recalescence effects.

Drop Specimen NT146

This specimen was melted in the levitation furnace, dropped in an atmosphere of 200 torr of helium, and gas quenched as it fell down the tube following recalescence. It has an actual composition of 25.3 at\% Ge and it undercooled 534 K ($\Delta T/T_m = 0.25$).

Figure 11 shows that the specimen has regions of fine and coarsened structures similar to NT008 except that only a trace of the specimen has the coarsened structure. Also, the size of the γ particles as shown in Figure 12 are smaller than those of NT008. Having a bimodal size distribution, the larger particles are about $2.8 \mu\text{m} \times 1.2 \mu\text{m}$ in size, and the smaller ones are $0.6 \mu\text{m} \times 0.4 \mu\text{m}$ in size. Both contain between 31 and 34 at% Ge.

Nb-25 at% Ge Liquid Quenched

Shown in Figure 13, this specimen was arc melted and then sprayed on a copper block. Here very fine γ particles can be seen comprising 35% of the volume with the balance being a continuous β phase. The particles again show a bimodal distribution in size; the larger ones being $0.4 \mu\text{m} \times 0.1 \mu\text{m}$, and the smaller ones $0.2 \mu\text{m} \times 0.05 \mu\text{m}$.

SUMMARY

Table 2 summarizes the analysis of the specimens. Each condition is unique in its own right. NT 008 having undercooled 450 K , clearly shows the effect of recalescence in that it shows regions of coarse dispersions amidst regions containing fine dispersions. The more coarsely dispersed regions have particle sizes approximately $1/3$ the size of the arc cast case but the compositions of the phases are similar to the arc cast case.

NT 146 undercooled about 534 K . The extra undercooling produced a microstructure further approaching the liquid quenched case although the particle size for liquid quenching is about 15% that of the drop tube specimen. Note however that the compositions of the phases are similar.

It is interesting to observe then that deeply undercooled bulk specimens can be obtained by containerless processing that are similar morphologically to liquid quenched specimens where one is restricted to a very thin sheet as a final product. In this context it would appear that, at least in this alloy system where the density of the phases is about the same, that the principal effect of a microgravity environment would be to provide conditions where a containerless process on a large scale is relatively easy to achieve. Such a characteristic then could be a major advantage of microgravity in producing unique bulk alloys.

REFERENCES

1. L. L. Lacy, M. B. Robinson, T. J. Rathz, N. D. Evans and R. J. Bayuzick, in "Materials Processing in the Reduced Gravity Environment of Space," edited by G. E. Rindone (Elsevier Science Publishing Co., New York, 1982), p. 87.
2. L. L. Lacy, T. J. Rathz, and M. B. Robinson, *J. Appl. Phys.* 53, 682 (1982).
3. L. L. Lacy, M. B. Robinson, and T. J. Rathz, *J. Cryst. Growth* 51, 47 (1981).
4. M. B. Robinson, M. S. Thesis, University of Alabama in Huntsville, 1981; NASA Report TM-82423, May 1981.
5. D. B. Wallace, Report on NASA/ASEE Summer Faculty Research Program, 1981.
6. Zemansky, M. W., Heat and Thermodynamics, 5th Edition (McGraw-Hill Book Co., New York, 1968).
7. J. H. Perepezko and D. H. Rasmussen, *Met Trans* 9A, 1490 (1978).
8. R. Mehrabian, *Intl. Metals Reviews*, 27, 185 (1982).
9. J. P. Hirth, *Met. Trans.* 9A, 401 (1978).
10. "Handbook of Tables for Applied Engineering Science, 2nd Edition", edited by R. E. Bolz and G. L. Ture (CRC Press, Cleveland, Ohio, 1973).
11. F. M. White, "Viscous Fluid Flow" (McGraw-Hill Book Co., New York, 1974) p. 209.
12. F. P. Incropera and D. P. DeWitt, "Fundamentals of Heat Transfer" (John Wiley & Sons, New York, 1981) p. 342.

TABLE 1

Hypercooling Temperatures for Selected Metals

Element	T_m (K)	ΔH (J/mole)	T^* (K)	T^*/T_m
Al	933	10,669	364	0.39
Cu	1356	13,453	429	0.32
Ni	1726	18,128	471	0.27
Fe	1808	15,305	366	0.20
Pt	2045	21,957	583	0.28
Nb	2741	26,822	664	0.24

T_m , ΔH , C_p from CRC Handbook¹⁰

TABLE 2

Quantitative Analysis of Nb-Ge Alloys

Specimen Type	β Composition at% Ge	γ Composition at% Ge	v/o γ	γ Size μm
Arc Cast	19.8	35.0	33 3	38.8 x 9.4 5.4 x 3.7
NT 008A(1)	22.0	35.0	41	4.6 x 1.5
NT 008B	20.5	36.4	31	13.8 x 3.6
NT 146	21.3 to 24.5	3.1 to 34.1	30	2.8 x 1.2 0.6 x 0.4
Liquid Quenched	23(2)	30.5 to 32.0(2)	34	0.4 x 0.1 0.2 x 0.05

1. A corresponds to the dark regions in Figure 9. B corresponds to the light regions.
2. Because of the extremely fine structure these compositions are only nominal. Accurate determinations will eventually be made by use of analytical transmission electron microscopy.

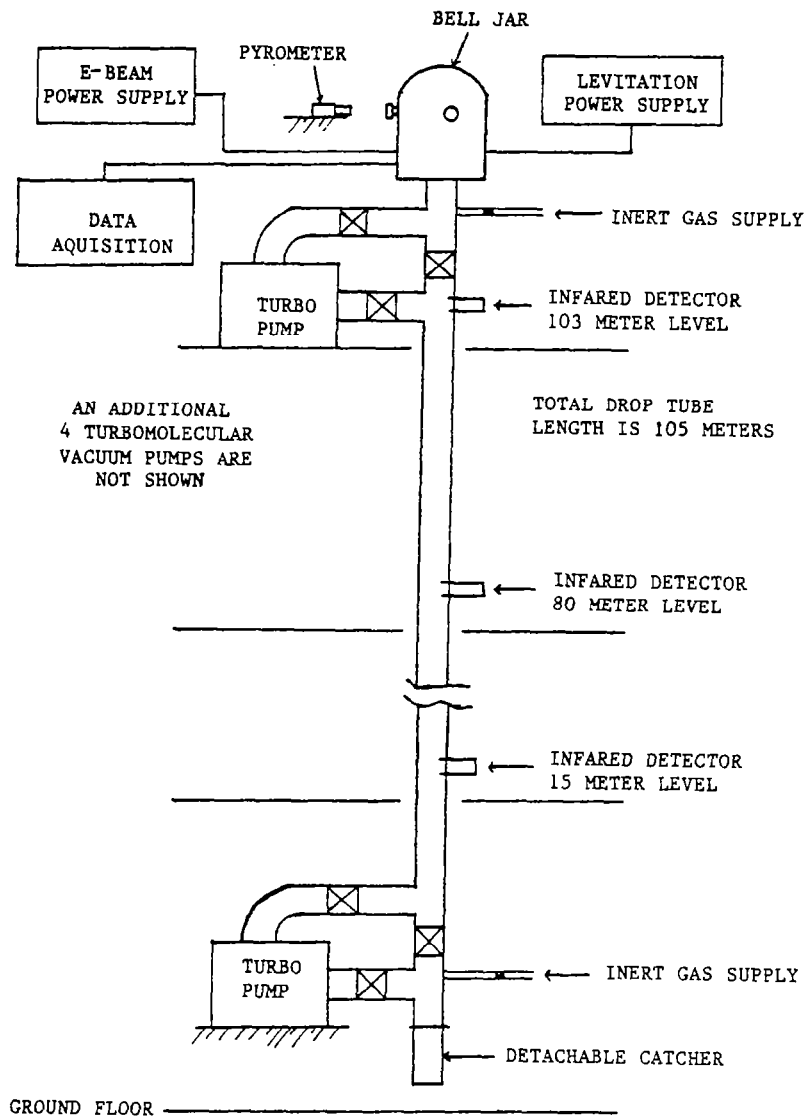


Figure 1. The 100 meter drop tube.

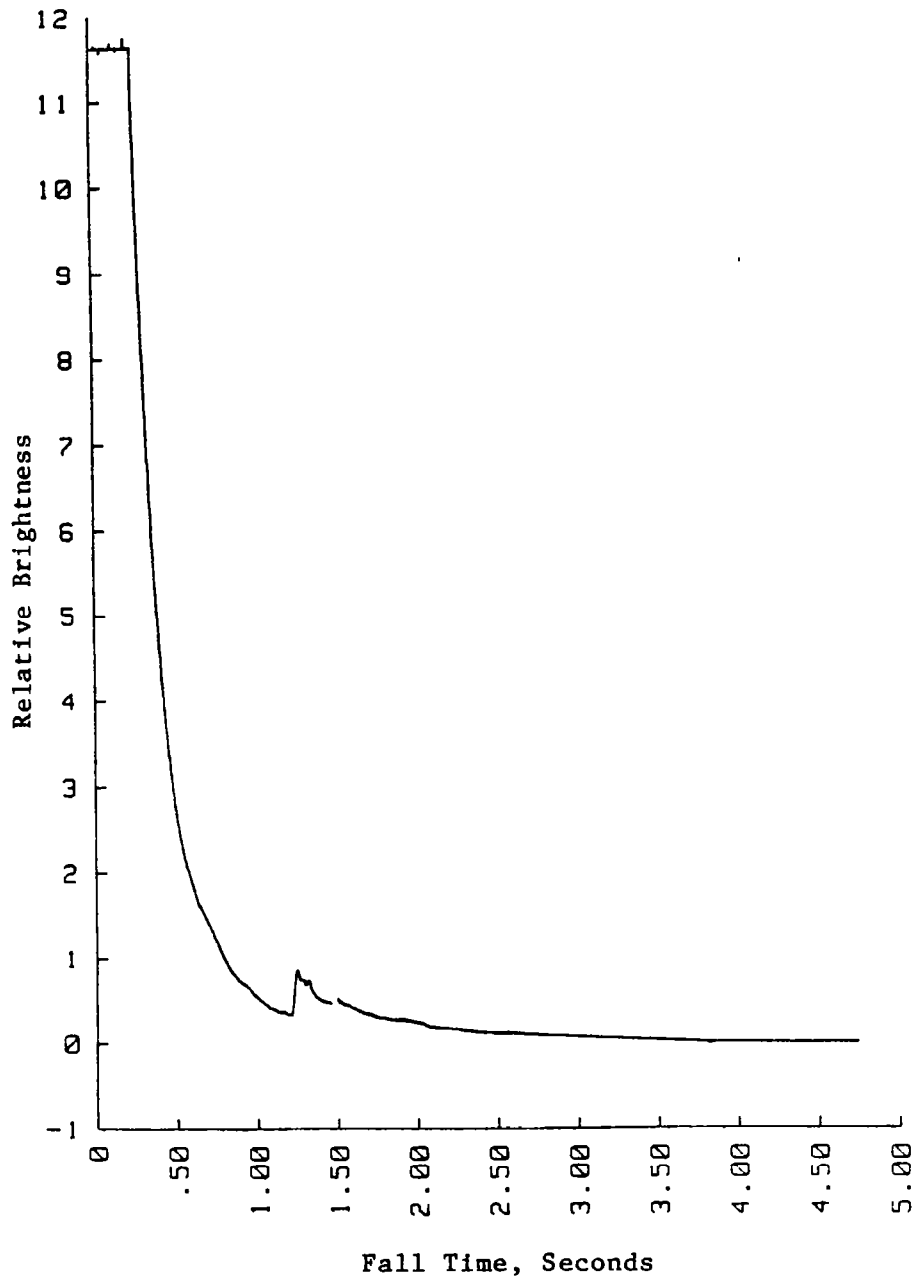


Figure 2. Example of a brightness curve for a Nb-Ge specimen.

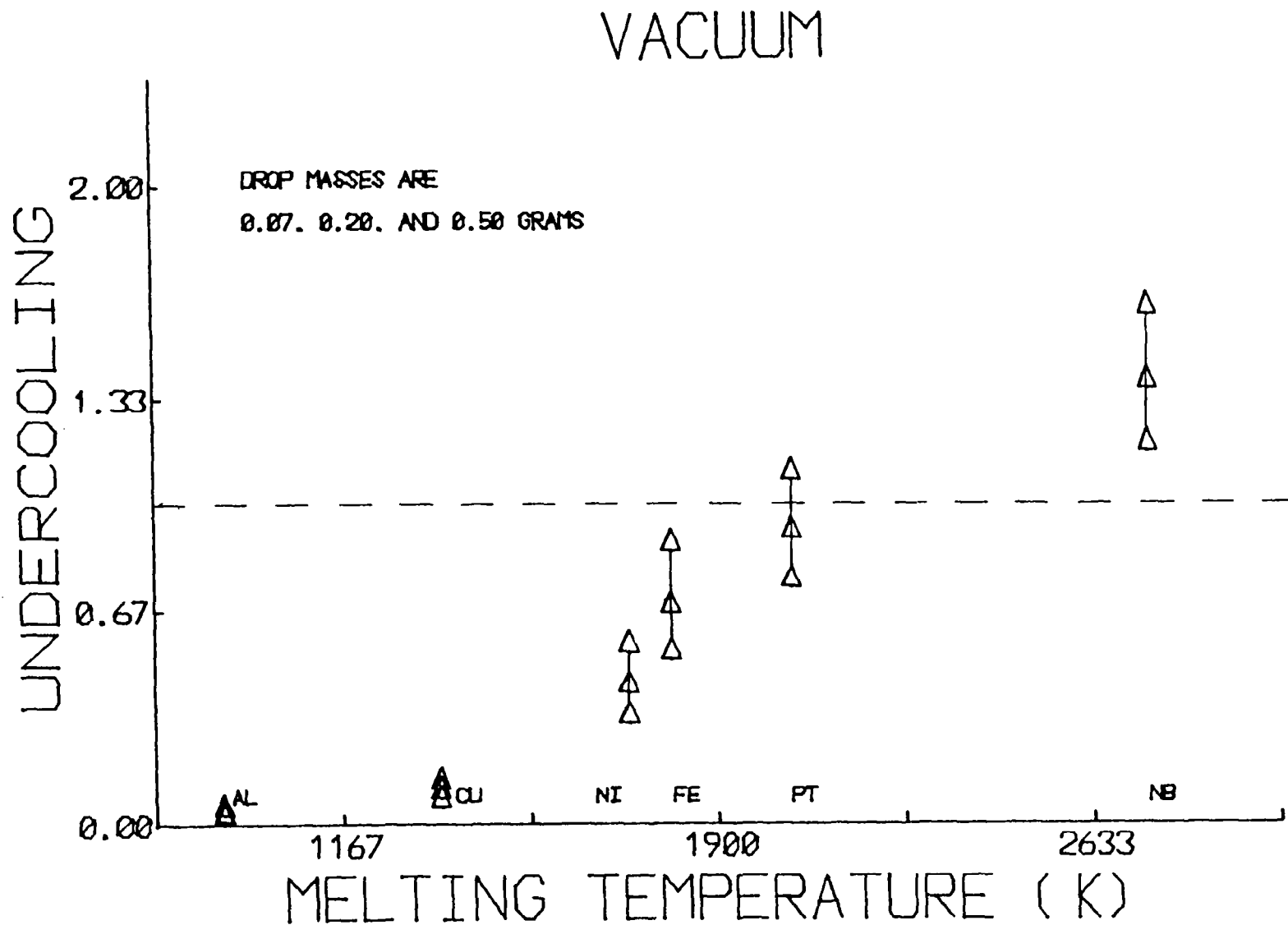


Figure 3. Maximum possible undercooling in vacuum for selected metals in the 100 meter drop tube.

200 TORR HE

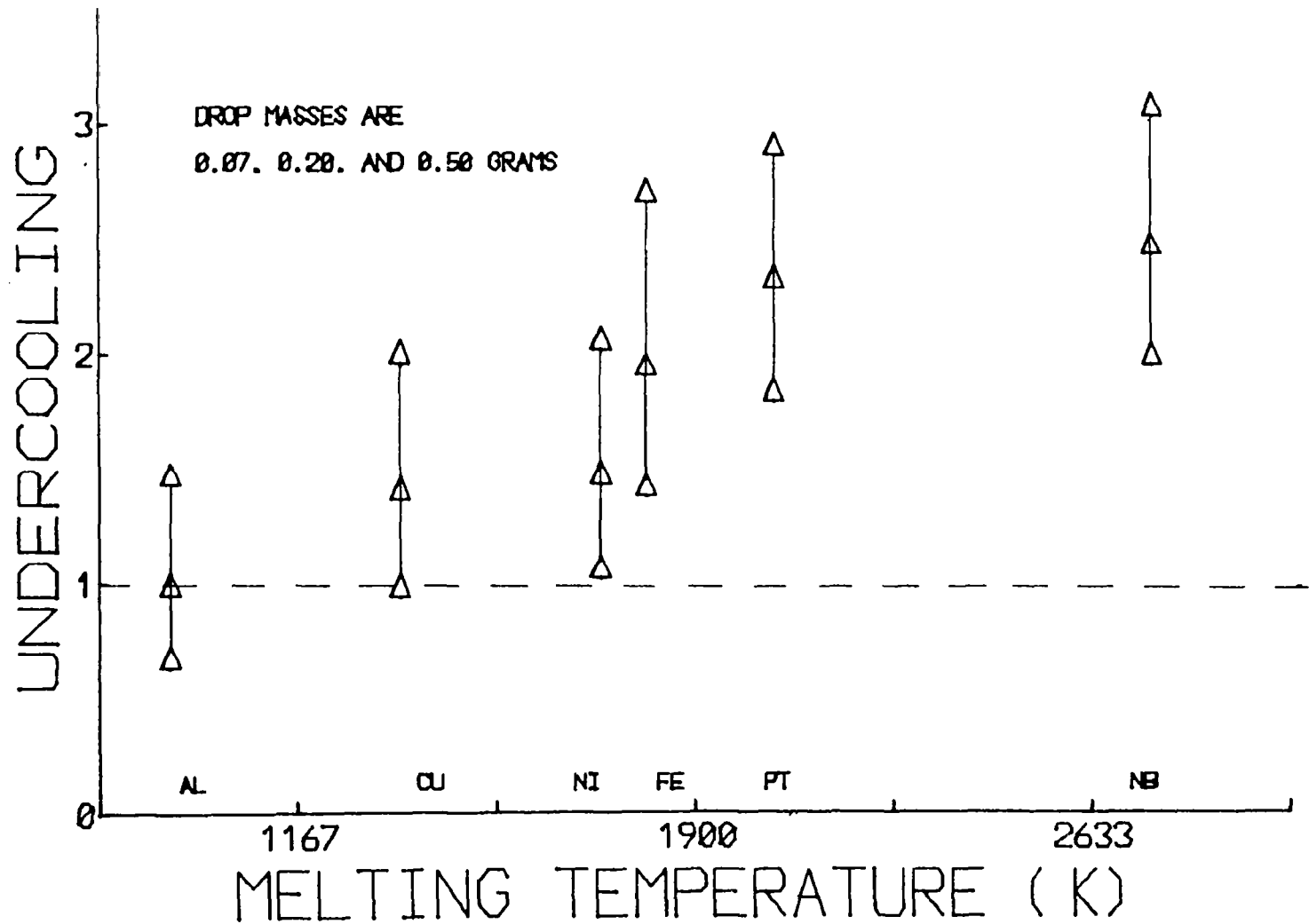


Figure 4. Maximum possible undercooling in 200 torr He for selected metals in the 100 meter drop tube.

760 TORR HE

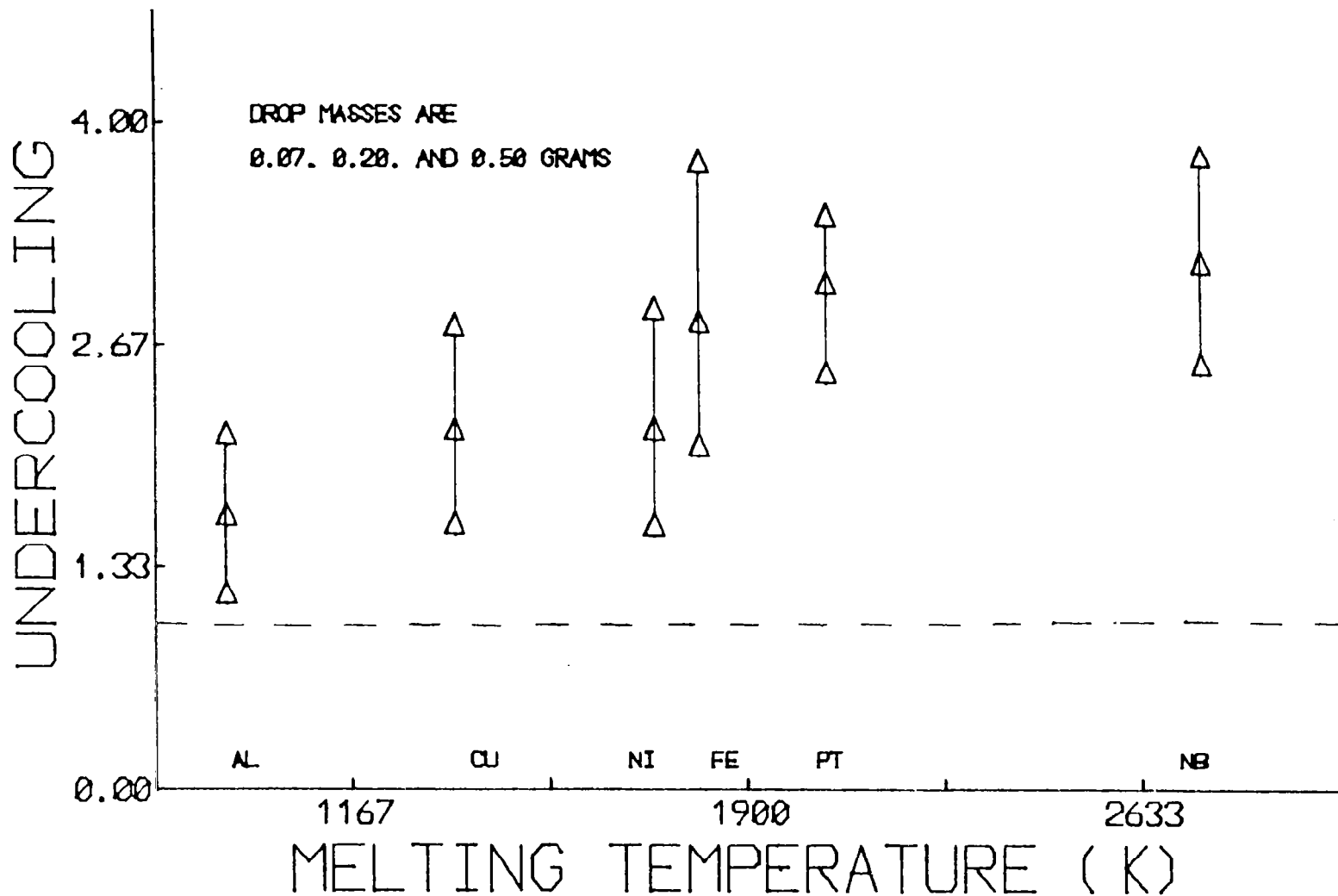


Figure 5. Maximum possible undercooling in 760 torr He for selected metals in the 100 meter drop tube.

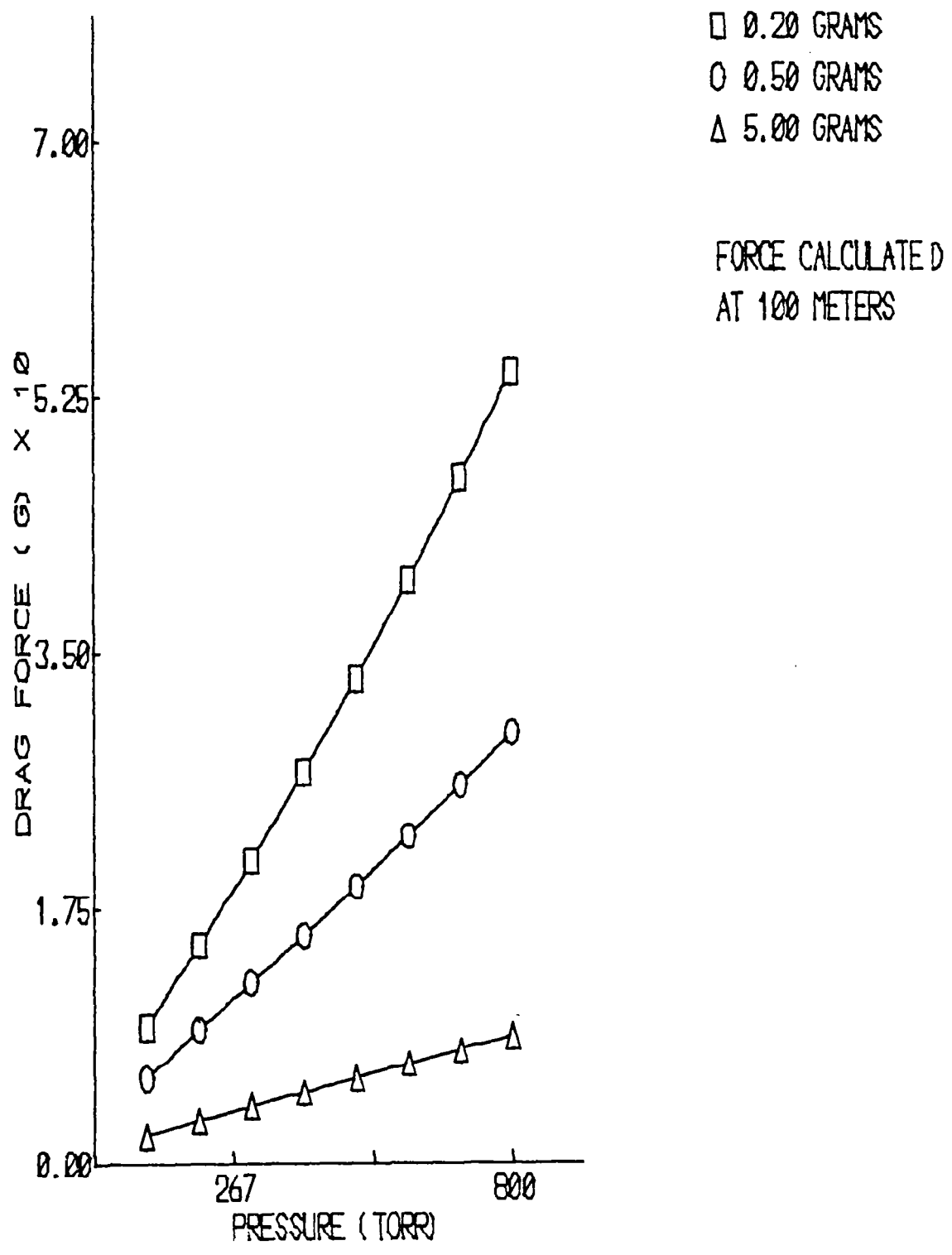


Figure 6. Drag force on various size Nb-27 at% Ge drops.

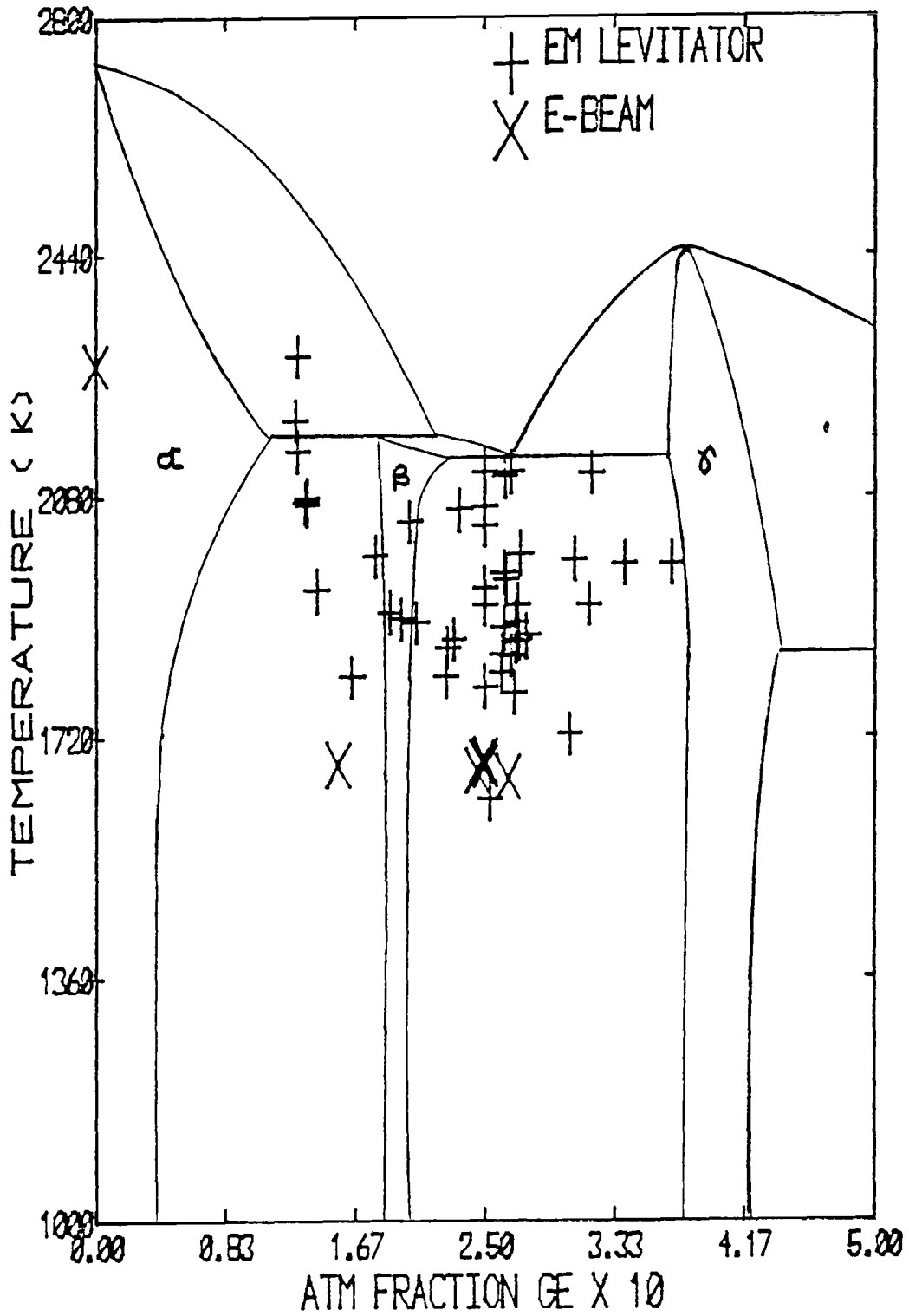


Figure 7. Summary of undercooling experience with the Nb-Ge binary system.

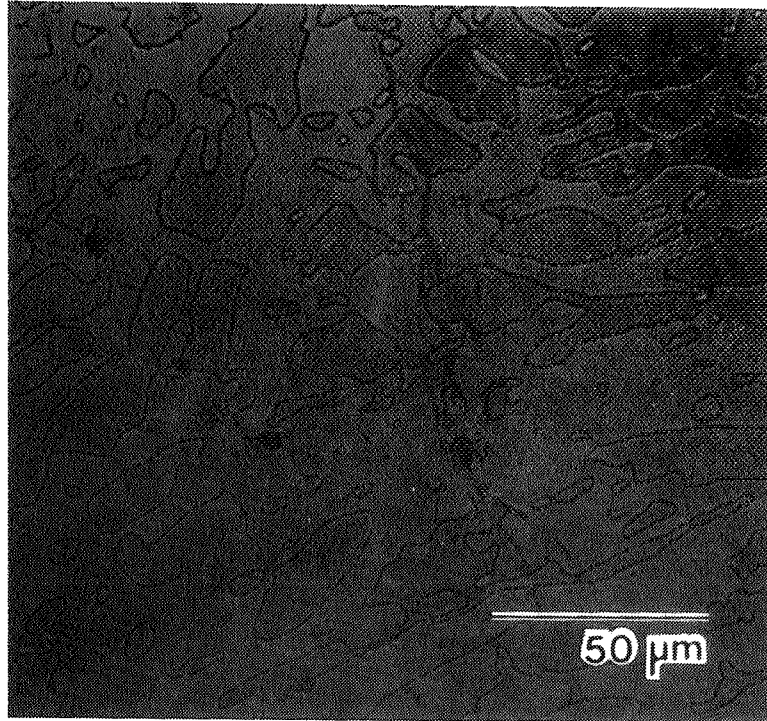


Figure 8. Arc cast microstructure of Nb-25 at% Ge.

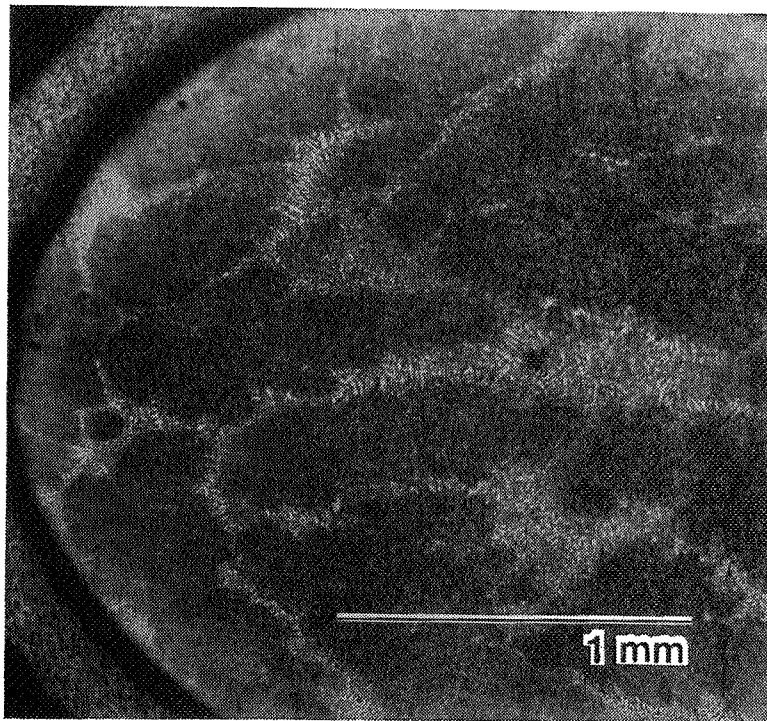


Figure 9. Micrograph of NT 008 where undercooling was 450 K.

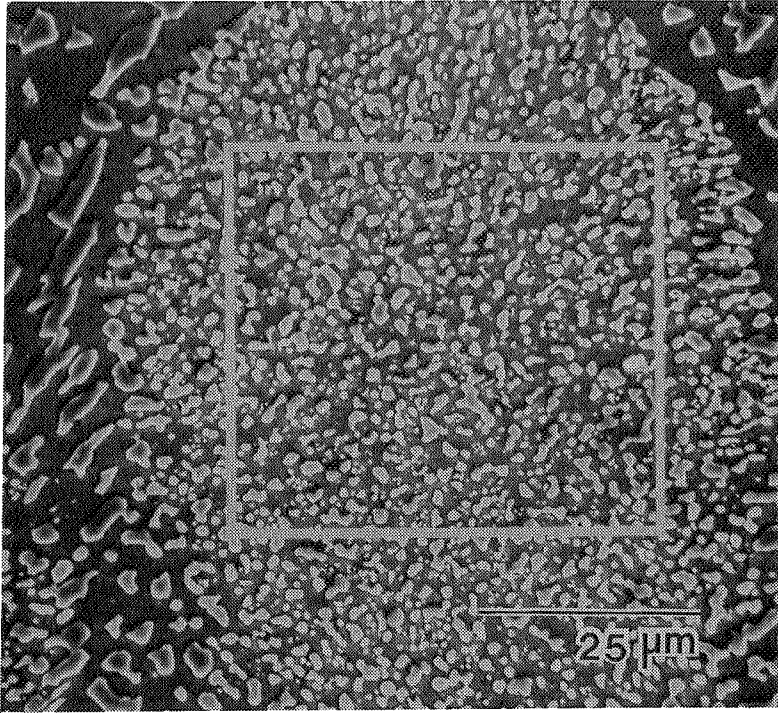


Figure 10. Microstructure of the fine regions in NT 008.

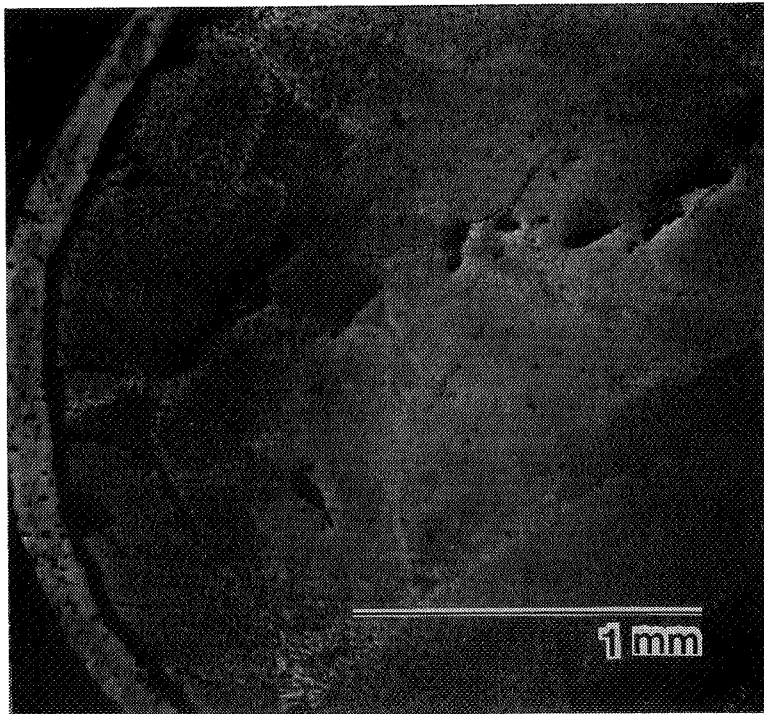


Figure 11. Macrograph of NT 146 where undercooling was 534 K.

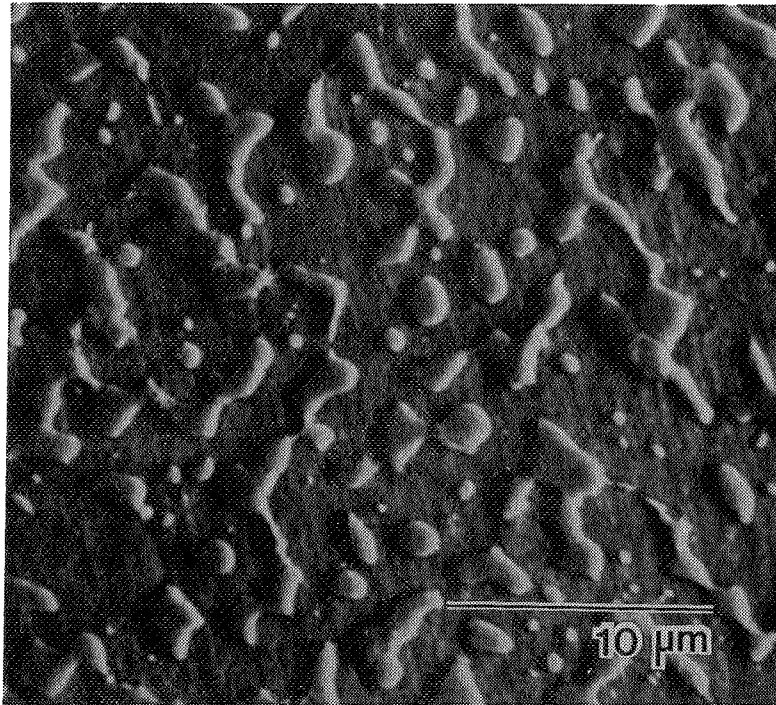


Figure 12. Microstructure of the fine regions in NT 146.

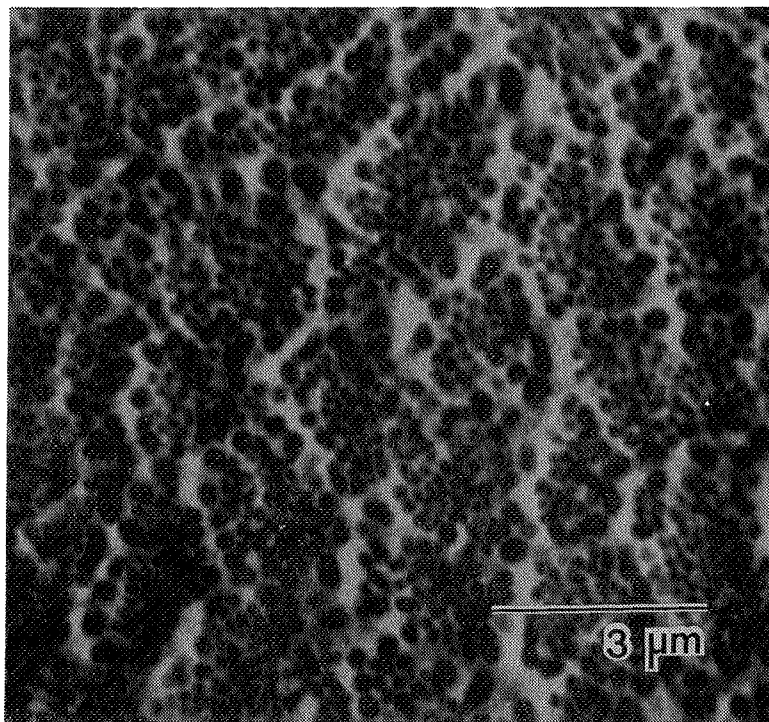


Figure 13. Microstructure of liquid quenched Nb-25 at% Ge.